

Locational Marginal Pricing based Smart Charging of Plug-In Hybrid Vehicle Fleets

Marina González Vayá, Göran Andersson
Power Systems Laboratory

ETH Zürich (Swiss Federal Institute of Technology Zürich)
{gonzalez,andersson}@eeh.ee.ethz.ch

1 Introduction

The electrification of transportation is becoming an increasingly important topic due to geopolitical concerns regarding the supply of oil and strategies against climate change. Plug-in-hybrid electric vehicles (PHEVs), which rely mainly on electricity for propulsion and are equipped additionally with a combustion engine to bridge larger distances, would play a key role. However the introduction of battery vehicles poses significant challenges to the supply, transmission and distribution of electricity. Previous studies have focused on the impact of PHEVs on electric utilities [1, 2, 3], highlighting the importance of a controlled or "smart-charging" scheme.

In the absence of a controlled charging scheme, vehicles would typically start charging when arriving at a location where charging is possible, e.g. home or workplace. This would accentuate the already existing peaks in electricity demand potentially leading to overloaded network assets and increasing generation costs. Vehicles being parked most of the time, load shifting is often possible: There is a certain time frame where the demand of these loads can be considered to be elastic. Simple dual tariff schemes could help shift the load initially, but wouldn't be viable at larger penetrations as new demand peaks could be created at the beginning of the low-tariff period. A large scale introduction of battery vehicles requires schemes with endogenous prices where the impact of the new load on electricity prices is taken into account. The smart charging scheme proposed here is based on day-ahead Locational Marginal Pricing, where fleet aggregators would participate in electricity markets placing demand bids. Charging is scheduled so as to minimize generation costs taking into account network constraints and the battery state of charge (SOC) constraints of the vehicles, which are given by their individual driving behavior. A multi-agent transport simulation called MATSim is used to forecast the driving patterns of individual vehicles [4]. The optimization framework adopted is an Optimal Power Flow (OPF): that is a welfare maximizing dispatch of loads and generators taking into account network constraints. This is an appropriate tool as the interdependencies between supply, demand and infrastructure are taken into account simultaneously. Thus the impact of PHEVs on the electricity market and network assets can be assessed. The proposed method has been tested with case studies on the Swiss system (comprising supply and demand of electricity and the transmission grid). The results show that this method leads to reduced generation costs and system stress. Moreover it can be used for system planning purposes as the impact of PHEV load on the different network assets can be assessed quantitatively.

This paper is structured as follows: First the simulation model will be illustrated in the following section. The results of the case studies are shown in section 3. Finally section 4 concludes the paper.

2 Model description

The aim of the proposed smart charging scheme is to charge the vehicles in a way that is optimal for the system, that is in a way that generation costs for the period under consideration (24 hours) are minimized. At the same time the bottlenecks of the transmission network and the state of charge constraints that arise due to the driving behavior are taken into account. As this is an intertemporal problem, a multiperiod optimization is required. However, it would be computationally prohibitive

to model every vehicle individually in such a multiperiod framework, for this reason the batteries of the vehicles at each network node are aggregated and modeled as a virtual battery, whose capacity, energy content and lower bound depend on the behavior of vehicles (arrival and departure time, energy consumption) and on the charging. Based on the outcomes of the multiperiod optimization, a sequential single-period OPF is performed where vehicles are modeled individually and the demand bids of the aggregated fleets at each node are defined in such a way that both models lead to the same outcome whenever this is possible.

Figure 1 gives an overview of the simulation framework:

- First, an agent-based transport simulation is performed [4], which results in departure and arrival times for each vehicle and an energy consumption for each trip. This information is used to shape the battery constraints of the multiperiod model and the demand bids of the single-period model.
- Second, the multiperiod OPF is performed, which determines the demand setpoints, price and quantity, for the single-period model. In this model vehicles are modeled as virtual batteries.
- Third, the sequential single-period model is run, leading to nodal prices, line loadings, charging profiles and generation for each time step. In this model each vehicle's state of charge evolution over time is modeled individually.

The later steps will be explained in detail the following subsections.

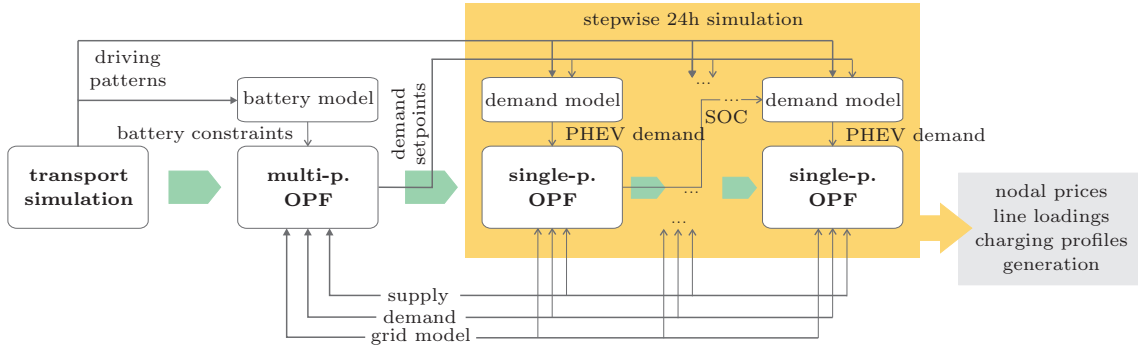


Figure 1: Structure of the simulation model

2.1 Multiperiod Optimal Power Flow

In the following the multiperiod optimization problem will be described. For this purpose the PHEV fleet is modeled as a set of aggregated storage resources which have special constraints due to vehicles' driving needs. The capacity and energy content of these storage resources change over time as vehicles depart/arrive from/to the different nodes.

The optimization routine determines the power supply and demand at each time step ($P_{G_i}^{(t)}$ and $P_{L_j}^{(t)}$ resp.) that minimize generation costs for the whole period under observation.

$$\min_{P_{G_i}^{(t)}, P_{L_j}^{(t)}, E_{VB_j}^{(0)}} \sum_{t=1}^T \sum_i \frac{1}{2} (m_{G_i} \cdot P_{G_i}^{(t)} + n_{G_i}) \cdot P_{G_i}^{(t)} \quad (1)$$

Subject to the following constraints:

$$\sum_i P_{G_i}^{(t)} = \sum_j P_{L_j}^{(t)} \forall t \quad (2)$$

$$P_{G_i, min} \leq P_{G_i}^{(t)} \leq P_{G_i, max} \forall t, i \quad (3)$$

$$P_{L_j,ref}^{(t)} \leq P_{L_j}^{(t)} \leq P_{L_j,ref}^{(t)} + \sum_{V_k \in \Omega_{L_j}^{(t)}} P_{V_k,conn} \forall t, j \quad (4)$$

$$|\sum_n PTDF_{n,l_m} \cdot (P_{G_i \in \Omega_n}^{(t)} - P_{L_j \in \Omega_n}^{(t)})| \leq P_{l_m,max} \forall t, l \quad (5)$$

$$E_{VB_j,min}^{(t)} \leq E_{VB_j}^{(t)} \leq E_{VB_j,max}^{(t)} \forall j, t \quad (6)$$

$$E_{VB_j}^{(0)} = E_{VB_j}^{(T)} \forall j \quad (7)$$

The objective function is defined by Equation (1) as a quadratic cost function where m_{G_i} and n_{G_i} are the slope and the intercept of the supply curve of a particular generator G_i respectively. Equation (2) represents the power balance constraint: the sum of the generated power P_{G_i} must equal the sum of power consumed P_{L_j} at each time step t . As a DC power flow formulation was used here, transmission losses are neglected. Equation (3) captures the lower and upper generation constraints of each power plant G_i . Similarly Equation (4) sets the upper and lower limits on the electricity demand at each load node L_j . The lower bound is the reference load $P_{L_j,ref}$, that is the load without PHEVs. This load is considered to be inelastic in this short-run (day-ahead) perspective. The upper bound is determined by the reference load plus the sum of charging capacities $P_{V_k,conn}$ of all vehicles connected to a particular node. Equation (5) states that the line limits should not be exceeded by the absolute values of the line flows, which are calculated using Power Transfer Distribution Factors (PTDFs)[5]. Additional constraints are needed to set limits to the stored energy in the virtual battery $E_{VB_j}^{(t)}$ and to set the initial value $E_{VB_j}^0$ of this variable equal to its final value $E_{VB_j}^{(T)}$. Equation (1) tells us that the initial energy content of the virtual batteries has been defined as an optimization variable. However, a fixed value for this parameter could be introduced easily if suitable. This optimization can be formulated as a quadratic program.

The upper battery bound $E_{VB_j,max}^{(t)}$ is given by the sum of capacities of all vehicles connected to a certain node.

$$E_{VB_j,max}^{(t)} = \sum_{k \in \Omega_j^{(t)}} C_{V_k,batt} \quad (8)$$

The lower battery bound of an individual vehicle is given either given by its minimum state of charge or by its required state of charge before departure ($SOC_{V_k,min}$ and $SOC_{V_k,req}$ respectively). These are aggregated at each network node to form $E_{VB_j,min}^{(t)}$.

$$E_{VB_j,min}^{(t)} = \sum_{k \in \Omega_j^{(t)}} \max(SOC_{V_k,min}, SOC_{V_k,req}) \cdot C_{V_k,batt} \quad (9)$$

The content of a virtual battery at any point in time is given by its content in the previous time step, the charging power ($P_{L_j}^{(t)} - P_{L_j,ref}^{(t)}$), the average battery charging efficiency of the fleet $\bar{\eta}_{j,char}$ and the negative and positive contribution of PHEVs departing and arriving at the given node ($E_{VB_j,dep}^{(t)}$ and $E_{VB_j,arr}^{(t)}$ respectively).

$$E_{VB_j}^{t+1} = E_{VB_j}^{(t)} + (P_{L_j}^{(t)} - P_{L_j,ref}^{(t)}) \cdot \Delta t \cdot \bar{\eta}_{j,char} - E_{VB_j,dep}^{(t)} + E_{VB_j,arr}^{(t)} \quad (10)$$

An example of the development of the characteristics of the virtual battery over time is shown in Figure 2. This example represents a fleet of 1 million vehicles which drive from home to work and back. It can be seen that the capacity of the virtual battery decreases dramatically during the time where vehicles are driving to work in the morning and home in the evening. It can also be seen that the lower bound increases before departure because the vehicles have to depart with enough energy in their batteries to bridge the next trip ($SOC_{V_k,min} < SOC_{V_k,req}$ holds for many vehicles).

The optimization results in a given load profile for the PHEV fleet as well as in nodal prices. Nodal prices are derived from the lagrangian multipliers of the equality constraint in Equation (2) and the inequality constraint in Equation (5) ($\lambda_{balance}$ and λ_{line} respectively) with the help of the PTDF factors.

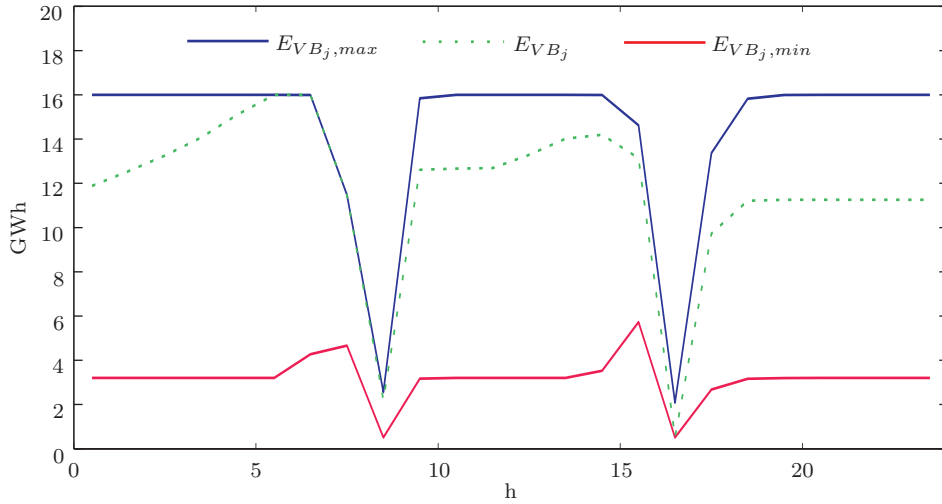


Figure 2: Virtual battery characteristics for a fleet of one million vehicles with 16 kWh batteries assuming ubiquitous charging and home-work-home driving patterns

$$p_n^{(t)} = \lambda_{balance}^{(t)} + \sum_{l_m} PTDF_{n,l_m} \cdot \lambda_{l_m,line}^{(t)} \quad (11)$$

From Equation (11) it is clear that the network nodes will have different prices only if there is a congestion, that is when constraint (5) is active.

2.2 Single-period Optimal Power Flow

The multiperiod optimization determines a dispatch schedule for the virtual batteries, but does not provide any information on individual PHEV charging and individual constraints. This is why a further step with the more detailed single-period optimization is needed. Consequently, actual PHEV charging might have to deviate from the optimum charging obtained in the multiperiod optimization.

At each time-step three tasks are performed sequentially, which will be illustrated in the following (see Figure 1):

- Determining vehicles' demand curve at each network node
- Performing an optimal power flow
- Allocating aggregate demand to individual vehicles and updating individual SOC's

Under the single-period OPF framework generators and loads place demand and supply bids. In a further step the Independent System Operator takes these bids and clears the market by maximizing social welfare while obeying network constraints implicitly. The demand bids are assumed to be linear. Their slope $m_{L_j}^{(t)}$ and intercept $n_{L_j}^{(t)}$ are set so that they correspond to the clearing quantities and prices of the multiperiod model ($P_{L_j \in \Omega_n, mp}^{(t)}$ and $p_{n, mp}^{(t)}$).

$$m_{L_j \in \Omega_n}^{(t)} \cdot P_{L_j \in \Omega_n, mp}^{(t)} + n_{L_j \in \Omega_n}^{(t)} = p_{n, mp}^{(t)} \quad (12)$$

However, there are deviations from the desired cost minimizing outcome calculated by the multiperiod model whenever:

- $P_{L_j, min}^{(t)} > P_{L_j, mp}^{(t)}$: too many batteries approaching their lower bound of the SOC
- $P_{L_j, max}^{(t)} < P_{L_j, mp}^{(t)}$: too many batteries approaching their upper bound of the SOC

Given nodal demand and supply curves, the optimization algorithm determines nodal generation P_{G_i} and load P_{L_j} values that maximize total welfare, i.e. the sum of consumer and producer surplus:

$$\max_{P_{G_i}, P_{L_j}} \sum_j \underbrace{\frac{1}{2} (m_{L_j} \cdot P_{L_j} + n_{L_j}) \cdot P_{G_i}}_{\text{demand (load)}} - \sum_i \underbrace{\frac{1}{2} (m_{G_i} \cdot P_{G_i} + n_{G_i}) \cdot P_{G_i}}_{\text{supply (generation)}} \quad (13)$$

Subject to the constraints:

$$\sum_i P_{G_i} = \sum_j P_{L_j} \quad (14)$$

$$P_{G_i, \min} \leq P_{G_i} \leq P_{G_i, \max} \forall i \quad (15)$$

$$P_{L_j, \min} \leq P_{L_j} \leq P_{L_j, \max} \forall j \quad (16)$$

$$|\sum_n PTDF_{n, l_m} \cdot (P_{G_i \in \Omega_n} - P_{L_j \in \Omega_n})| \leq P_{l_m, \max} \forall l \quad (17)$$

Equations (14)-(17) correspond to the constraints already discussed in the multiperiod case: power balance, generation bounds, demand bounds and line limits.

The market clearing leads to aggregated consumption values, which are allocated to the individual vehicles according to the urgency of the charging. The parameters taken into account to quantify this are:

- the time until the departure of the vehicle compared with the time necessary to charge up to de desired level and
- the actual state of charge compared with the desired state of charge.

Finally the SOC of each individual vehicle is updated and the next time step can be simulated.

3 Swiss Model Case Studies

To verify the suitability of the proposed scheme several case studies were carried out. Three scenarios were simulated:

- **Reference scenario**, that is the status quo previous to the introduction of PHEVs.
- **Uncontrolled charging**, where vehicles start charging whenever they arrive at their destination until their batteries are full or they depart for the next trip.
- **Smart charging**, which has been described in the previous section.

A fleet of 1 million PHEVs was modeled, which corresponds to penetration of about 25% [6]. The PHEV parameters used are displayed in Table 1.

The simulations were performed on a model of the Swiss transmission grid (220kV and 380kV voltage levels) provided by Swissgrid, the Swiss Transmission System Operator. The system comprises 191 lines, 246 network nodes and 21 transformers between the voltage levels 220kV and 380kV. Furthermore data was collected on over 130 Swiss power plants [7]. Load data was obtained from the yearly Swiss electricity statistics [8] and distributed among the different network nodes according to the size of the underlying population. Although this is only an approximation, there is usually a high correlation between load and population size [9].

battery capacity	minimum SOC	charge efficiency	connection capacity
$C_{V_k, batt}$	$SOC_{V_k, min}$	$\eta_{V_k, char}$	$P_{V_k, conn}$
16 kWh	0.2	0.9	3.5 kW

Table 1: PHEV parameters

Figure 3 shows the reference load, defined here as the domestic load plus the exports minus the imports, for a winter day (16.12.2009 as shown in [8]). The winter load was chosen because it is higher than in the other seasons, so it represents a more critical situation. Imports and exports are exogenously given and correspond to the same winter day [8]. Figure 3 also illustrates how the demand is supplied by the different types of power plants according to the OPF dispatch. The simulation results are very similar to the actual generation structure shown in [8]. The total load profiles (reference load and PHEV load) resulting from the different scenarios are depicted in Figure 4. In the uncontrolled charging scenario vehicles start charging as soon as they arrive to their destination. It can be seen that this accentuates the already existing peaks in electricity demand. On the other hand the smart charging scenarios present a flatter demand profile. Most charging takes place during the valley hours of the night, when demand and prices are the lowest. Some charging takes place during daytime because some vehicles need to charge to get back home from work. However, charging during demand peaks is successfully prevented. We can see that the actual charging profile under smart charging (single-period model) deviates slightly from ideal charging profile derived in the multiperiod optimization. The reasons for this were already mentioned in subsection 2.2.

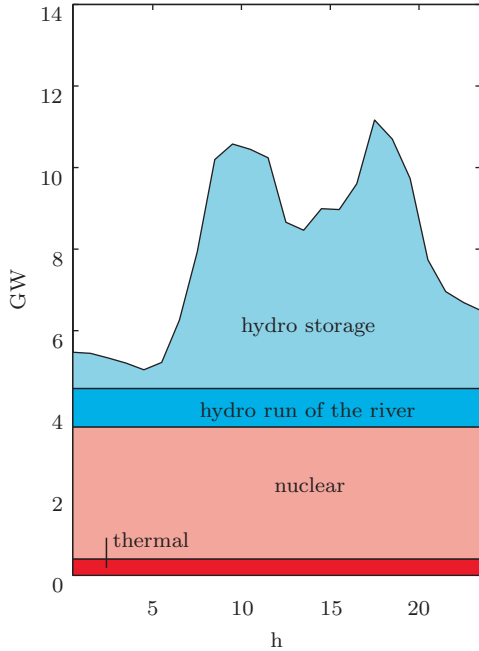


Figure 3: Reference load and generation structure

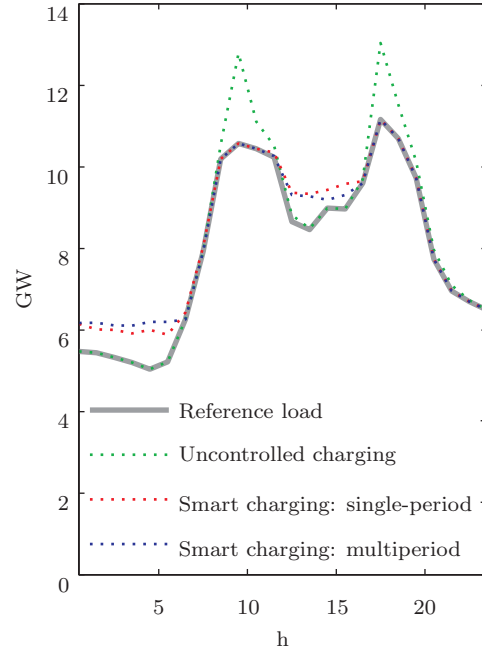


Figure 4: Scenario load profiles

The impact of the load profiles on the prices is shown in Figure 5. In the reference scenario, it can be seen that there is only congestion during peak hours. The rest of the time there is a single price at all locations. The price profiles of the smart charging scenario are very similar to those of the reference scenario, except for the fact that prices increase slightly during the hours where charging takes place: the valley hours of the night and in between the two consumption peaks. Moreover, the prices during congestion remain unchanged, as no charging takes place here. Finally, it can be seen that uncontrolled charging leads to extreme prices during peak hours. This of course is also reflected in the generation costs: uncontrolled charging leads to a 8% increase in generation costs compared with the reference scenario while smart charging leads to a 7% increase. Although the difference might not seem high enough to justify the implementation of smart charging, the really crucial issue is the overloading of system assets, as will be discussed in the following.

Figure 6 depicts the normalized loading over time of a line and a transformer whose line constraint (Equation (17)) is violated under the uncontrolled charging scenario, i.e. they get overloaded.

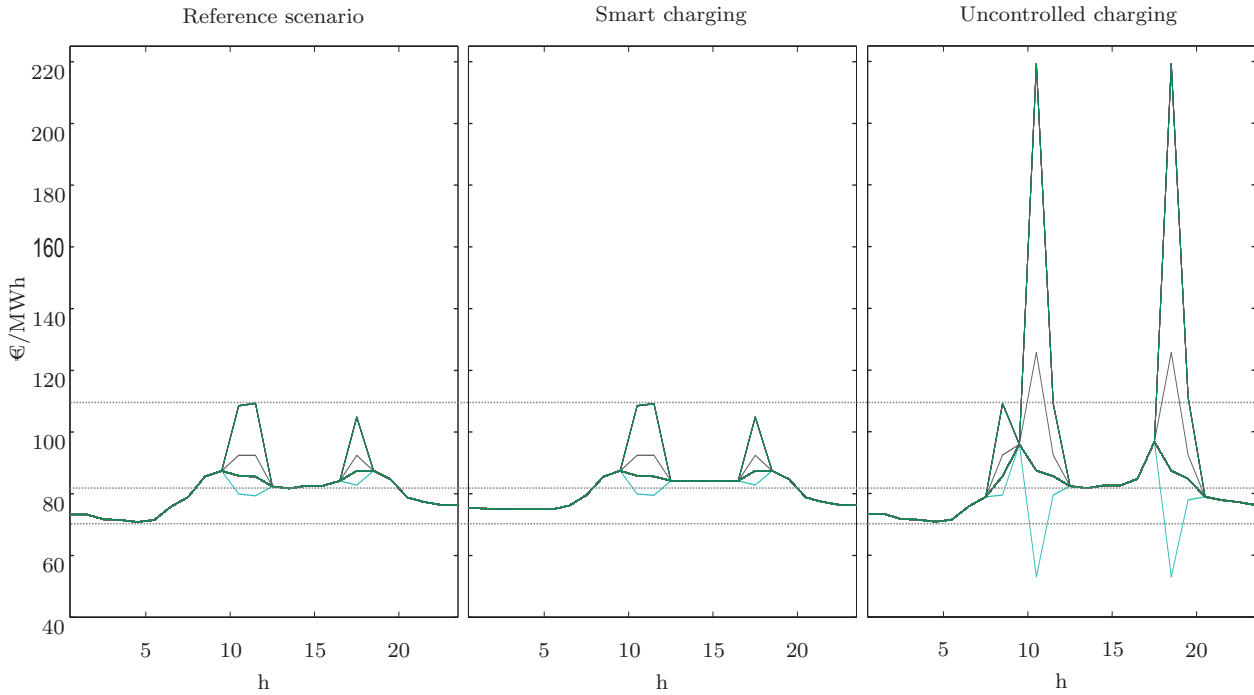


Figure 5: LMP profiles for the different scenarios

This means that uncontrolled charging would not be feasible at all without the reinforcement of the existing infrastructure. On the other hand, it can be seen that the smart charging scheme prevents this situation and so PHEVs can be successfully integrated.

4 Conclusion and Outlook

A large penetration of PHEVs would pose significant challenges to the power system infrastructure if no controlled charging strategy is implemented, accentuating the existing peaks in demand. However, vehicles can typically be characterized as flexible loads as they are driving only a small percentage of the time. This gives some scope for charging in a way that is beneficial for the system: that is in a way that minimizes generation costs and ensures that network assets are not overloaded.

An optimal dispatch based on Locational Marginal Prices has been proposed in this paper. First the cost minimizing charging profile is determined within a multiperiod OPF framework where vehicle fleets are modeled as virtual batteries. Second demand bids are placed accordingly within a sequential single-period OPF, where vehicles are modeled individually. The feasibility of the concept has been proven with case studies on the actual Swiss transmission grid with a large penetration of vehicles. Results have shown that the smart charging scheme proposed prevents charging during peak hours, reduces asset stress and generation costs. Moreover this model shows the impact of the additional load on transmission lines and could thus be used for planning purposes.

Further work will focus on the following improvements of the model:

- Market coupling with France, Germany, Austria and Italy so that cross-border flows are modeled endogenously.
- Modeling of the hydro storage power plants as an intertemporal problem.
- Stochastic OPF formulation specially taking into account the uncertainty about vehicle behavior.

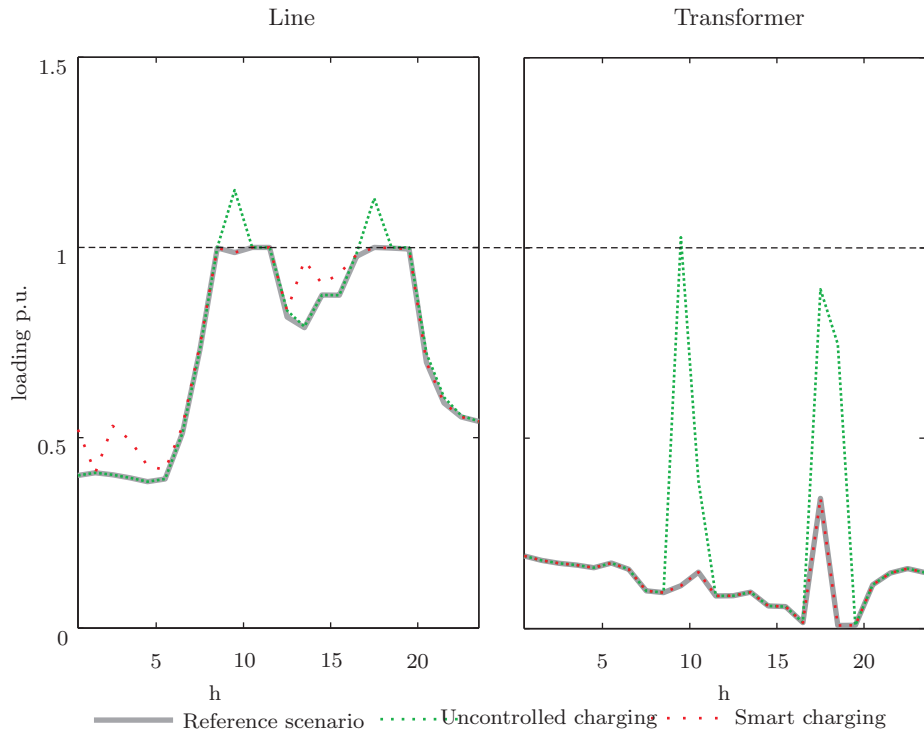


Figure 6: Loading profiles of overloaded line and transformer

Acknowledgements

The authors would like to thank Swissgrid for providing the data on the Swiss transmission grid. Moreover they would like to thank Rashid Waraich from the Institute for Transport Planning and Systems (ETH Zürich) for the transport simulations with MATSim.

This research was carried out within the project Technology-centered Electric Mobility Assessment, sponsored by the Competence Center for Energy & Mobility, SwissElectric Research and the Erdöl-Vereinigung.

References

- [1] S. W. Hadley. Evaluating the impact of plug-in hybrid electric vehicles on regional electricity supplies. In *Bulk Power System Dynamics and Control*.
- [2] K. Parks, P. Denholm, and T. Markel. Costs and emissions associated with plug-in hybrid electric vehicle charging in the Xcel Energy Colorado service territory. Technical report, National Renewable Energy Laboratory, 2007.
- [3] M. Kintner-Meyer, K. Schneider, and R. Pratt. Impacts assessment of plug-in hybrid vehicles on electric utilities and regional U.S. power grids. Part 1: Technical analysis. Technical report, Pacific Northwest National Laboratory, 2007.
- [4] M. Balmer, K.W. Axhausen, and K. Nagel. Agent-based demand-modeling framework for large-scale microsimulations. *Transportation Research Record: Journal of the Transportation Research Board*, 1985(2006):125–134, 2006.
- [5] F. L. Alvarado. Solving power flow problems with a Matlab implementation of the power system applications data dictionary. In *HICSS-32. Proceedings of the 32nd Annual Hawaii International Conference on System Sciences*, volume Track3.

- [6] Bundesamt für Statistik. *Mobilität und Verkehr 2010 (Swiss transportation statistics, in German)*. 2010.
- [7] Bundesamt für Energie. *Statistik der Wasserkraftwerkenanlagen der Schweiz (Swiss hydro power statistics, in German)*. 2010.
- [8] Bundesamt für Energie. *Schweizerische Elektrizitätsstatistik 2009 (Swiss electricity statistics, in German)*. 2010.
- [9] Zhou Qiong and J. W. Bialek. Approximate model of European interconnected system as a benchmark system to study effects of cross-border trades. *IEEE Transactions on Power Systems*, 20(2):782–788, 2005.